4-Aryl-1,2,3-triazole: A Novel Template for a Reversible Methionine Aminopeptidase 2 Inhibitor, Optimized To Inhibit Angiogenesis in Vivo

Lara S. Kallander,* Qing Lu, Wenfang Chen,‡ Thaddeus Tomaszek, Guang Yang,# David Tew, Thomas D. Meek, Glenn A. Hofmann, Christina K. Schulz-Pritchard, Ward W. Smith,|| Cheryl A. Janson,§ M. Dominic Ryan,⊥ Gui-Feng Zhang,⊗ Kyung O. Johanson, Robert B. Kirkpatrick, Thau F. Ho, Paul W. Fisher,▽ Michael R. Mattern,● Randall K. Johnson,△ Michael J. Hansbury,† James D. Winkler,◇ Keith W. Ward, Daniel F. Veber,£ and Scott K. Thompson

GlaxoSmithKline Pharmaceuticals, King of Prussia, Pennsylvania 19406

Received April 29, 2005

Abstract: Inhibitors of human methionine aminopeptidase type 2 (hMetAP2) are of interest as potential treatments for cancer. A new class of small molecule reversible inhibitors of hMetAP2 was discovered and optimized, the 4-aryl-1,2,3-triazoles. Compound **24**, a potent inhibitor of cobalt-activated hMetAP2, also inhibits human and mouse endothelial cell growth. Using a mouse matrigel model, this reversible hMetAP2 inhibitor was also shown to inhibit angiogenesis in vivo.

Inhibition of angiogenesis is considered a desirable pathway for stopping tumor growth and metastasis primarily because of the low potential for toxicity or resistance,[1] as well as the promise of treating a broad spectrum of tumor types.[2] Fumagillin (Figure 1, **1**), a natural product that exerts its antiangiogenic effects through the inhibition of endothelial cell proliferation,[3] was discovered to be an irreversible inhibitor of methionine aminopeptidase 2[4,5] (MetAP2) by covalently binding to His231.[6−8] There is evidence that the MetAP2 inhibition by fumagillin (and analogues)[4,9,10] is responsible for the observed antiangiogenic activity. Additional validation for MetAP2 as a target for cancer therapy was published more recently; a reversible bestatin-based MetAP2 inhibitor was shown to inhibit angiogenesis and suppress tumor growth.[11]

Human MetAP2 is one of two enzymes that catalyze the removal of N-terminal methionine residues from intracellular proteins. The enzyme is characterized by a bimetallic center activated by either cobalt[12] or manganese,[13] which is supported by residues that form a pita-bread shaped fold.[14] TNP-470,[15] a synthetic analogue of fumagillin, is a hMetAP2 inhibitor that has advanced to clinical trials[16,17] (Figure 1, **2**). This irreversible inhibitor is limited by its short half-life in serum and dose-limiting neurotoxicity. Reversible inhibitors are generally favored due to decreased likelihood of toxicity or immunogenic responses. Concurrent with our studies, reversible inhibitors based on fumagillin,[18] bestatin,[19] or a 1,2,4-triazole[13,20−22] template have been reported. In this report, we describe the discovery and optimization of 4-aryl-1,2,3-triazoles as reversible inhibitors of hMetAP2.

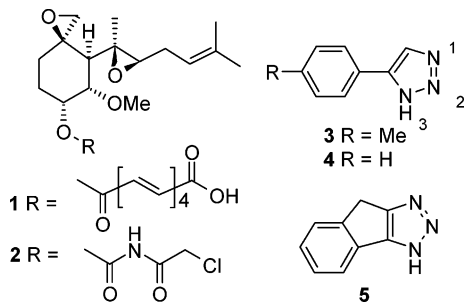

Figure 1. Structure of fumagillin (**1**), TNP-470 (**2**), and the hMetAP2 screening hits **3**, **4**, and **5**.

Scheme 1[a]

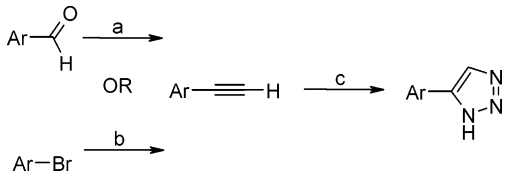

[a] Reagents, conditions, and yields: (a) $(MeO)_2P(O)CN_2C(O)CH_3$, K_2CO_3, MeOH, 71−99%; (b) TMSCCH, cat. $PdCl_2$, PPh_3, CuI, Et_3N, then MeOH, KOH, 63%; (c) $TMSN_3$, PhMe, reflux, then H_2O, 57−2%.

The 4-aryl-1,2,3-triazoles were prepared as described in Scheme 1. Our synthetic route made use of the availability of diversely substituted benzaldehydes, which were readily converted to terminal alkynes under mild conditions using a modified Corey−Fuchs homologation.[23] This method could also be applied to pyridylaldehydes, or alternatively, the ethynylpyridines were prepared from the corresponding bromopyridines through a Sonogashira cross-coupling reaction followed by basic hydrolysis of the trimethylsilyl group.[24] Cycloaddition with trimethylsilyl azide then formed the desired triazole derivatives after aqueous hydrolysis of the trimethylsilyl group.[25]

Our efforts began by screening our compound collection to identify inhibitors of cobalt-activated hMetAP2. Several potent inhibitors were discovered ($K_{i,app}$ < 100 nM) from a novel structural class, the 1,2,3-triazoles (Figure 1, **3**, **4**, and **5**). These compounds were surprisingly potent for very small molecules (MW < 160). A full kinetic analysis revealed that compound **3** is a reversible, competitive inhibitor with a K_i of 4.2 nM, IC_{50} = 10 nM (fumagillin IC_{50} = 1.2 nM in our cobalt-activated hMetAP2 assay). Compound **3** was found to be very selective for MetAP2 over other metallopro-

* To whom correspondence should be addressed. Phone: (610)-270-4814. Fax: (610)-270−4490. E-mail: lara.s.kallander@gsk.com.
‡ Current address: Finnegan Henderson et al., Palo Alto, CA.
# Current address: Tanabe Research Lab. USA, San Diego, CA.
|| Current address: Argonne National Laboratory, Argonne, IL.
§ Current address: Shamrock Structures, Woodridge, IL
⊥ Current address: Millennium Pharmaceuticals, Cambridge, MA.
⊗ Current address: Applied Molecular Evolution, San Diego, CA.
▽ Current address: Centocor Inc., Radnor PA.
● Current address: Progenra Inc., Malvern, PA.
△ Current address: Independent consultant, Santa Fe, NM.
† Current address: Incyte Corporation, Wilmington, DE.
◇ Current address: Array Biopharma Inc., Boulder, CO.
£ Current address: Independent consultant, Ambler, PA.

10.1021/jm050408c CCC: $30.25
Published on Web 08/06/2005

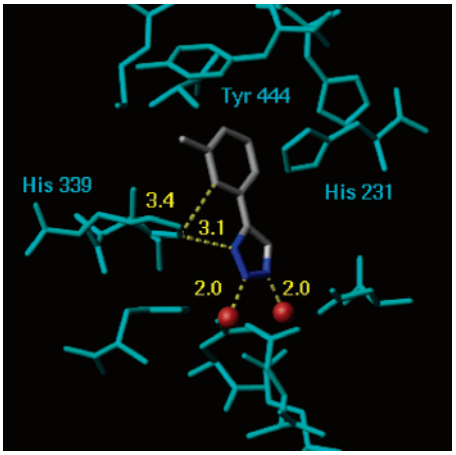

Figure 2. X-ray crystal structure of compound **18** (grey and blue) bound to hMetAP2 (turquoise). Cobalts are given in red. The atomic coordinates and structure factors (code 2ADU) have been deposited in the Protein Data Bank. (http://www.rcsb.org/). This figure was generated using the program MolMol.[26]

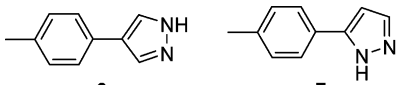

6 $K_{i,app}$ = 280 nM **7** 13% inhibition at 1 uM

Figure 3. hMetAP2 inhibitiory activity of pyrazoles.

teases such as MetAP1 (IC_{50} = 7100 nM) and matrix metalloprotease-9 (IC_{50} > 10 000 nM). Working within this chemical class, we wanted to improve the inhibitory potency and gain a structural understanding of the interaction of these compounds with the enzyme active site.

Concurrent with lead optimization, the X-ray cocrystal structure of compound **18** bound in the active site of hMetAP2 was solved at 1.9 Å resolution (Figure 2). This structure revealed that there is a key binding interaction between triazole nitrogens N-1 and N-2 and the active site cobalt atoms, similar to that noted in the crystal structure of a 1,2,4-triazole bound to cobalt-activated bacterial MetAP.[20] This tight coordination (interatomic distance 2.0 Å) probably accounts for much of the strong binding of these small molecules. The third triazole nitrogen appears not to be directly involved in binding to the metals but engages in a H-bond to His339.

To further explore whether N-1 and N-2 of the triazole contributed to the binding affinity of the compounds, pyrazole analogues of **3** were prepared. Replacing N-3 with carbon (Figure 3, **6**) led to a modest reduction in potency, suggesting a utility for 4-arylpyrazoles in the inhibition of metalloproteases such as MetAP2. However, replacing N-1 with carbon (**7**) significantly reduced the MetAP2 potency. These results provide further evidence that N-1 and N-2 in the heteroaryl ring are responsible for maintaining direct coordination with the active site metals and are thus important for inhibition.

The potent inhibitory activity of the tricyclic compound **5** suggested that there may be room in the active site for additional substitution at the 2-position of a 4-phenyl-1,2,3-triazole (Figure 1). Instead, the potency was shown to decrease as the 2-substituent increased in size from methyl to phenyl (compounds **8**−**10**, Table 1). This appears to indicate that the orientation of the

Table 1. hMetAP2 Inhibition Activity of 4-Aryl-1,2,3-triazoles[a]

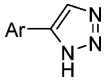

compd	Ar	$K_{i,app}$ (nM)
3	4-Me-phenyl	15
4	phenyl	70
5	as shown in Figure 1	52
8	2-Me-phenyl	112
9	2-OMe-phenyl	150
10	2-Ph-phenyl	>1000
11	4-Et-phenyl	30
12	4-*n*-Pr-phenyl	>1000
13	4-OH-phenyl	>1000
14	4-NH_2-phenyl	337
15	4-Cl-phenyl	6
16	4-Br-phenyl	3
17	4-I-phenyl	1
18	3-Me-phenyl	18
19	3-OH-phenyl	300
20	3-NH_2-phenyl	280
21	3-($PhCH_2NH$)phenyl	29
22	3-I-phenyl	16
23	3-Br-phenyl	4
24	3,4-di-Br-phenyl	1
25	2-benzofuran	13
26	2-pyridyl	41
27	3-pyridyl	260
28	4-pyridyl	>1000
29	6-Me-2-pyridyl	6
30	5-Me-2-pyridyl	3
31	4-Me-2-pyridyl	8
32	3-Me-2-pyridyl	52

[a] $K_{i,app}$ values were determined using the Dixon method assuming competitive inhibition for compounds of the same structural series.

aromatic ring relative to the triazole ring is important for binding; the coplanar orientation observed in the X-ray crystal structure may be preferred because it avoids steric crowding between the aromatic ring and His231.

A methyl group in the 4-position of a 4-phenyl-1,2,3-triazole enhances the enzyme inhibition 5-fold over the unsubstituted ring (**3**, **4**); however, compounds with chain lengths longer than ethyl were significantly less potent. A reduction in inhibition was also observed by introducing a hydroxy or an amino group in the same position (**13**, **14**). Analysis of the crystal structure indicates that Tyr444 may be responsible for the size limitations and hydrophobic nature of this area of the binding pocket. Significant improvements in potency via 4-substitution were achieved through the introduction of halogens (**15**−**17**).

The SAR for substitution at the 3-position of the aryl ring was generally similar to the corresponding 4-position, i.e., compounds with small hydrophobic groups demonstrated better inhibition than compounds bearing polar substituents such as hydroxy and amino. However, larger substituents were accommodated at the 3-position, as might be predicted based on the available space observed in the crystal structure. For example compound **21**, with a benzylamino substituent, shows good inhibitory potency. Again, the greatest enhancements in inhibition were obtained by introducing halogens, especially bromine, at the 3-position (**23**).

To take advantage of potency enhancements resulting from the introduction of halogens at the 3- and 4-position of the phenyl ring, a 3,4-dibromophenyl compound

Table 2. Enzymatic and Cellular Inhibition by 4-Aryl-1,2,3-triazoles

	enzyme $K_{i,app}$ (μM)		cellular IC_{50} (μM)[a]	
compd	Co^{2+}	Mn^{2+}	HUVEC	MS-1
3	0.015	4.4	30	20
15	0.006	11	5	20
16	0.003	11	6	20
17	0.001	0% inhibition at 20 μM	20	20
24	0.001	16	2	2
25	0.013	26% inhibition at 20 μM	20	30
30	0.003	15	2	3
31	0.008	14	>30	8

[a] IC_{50} was that concentration of compound that reduced cell viability to 50% of control (untreated) viability, as determined from plots of concentration vs percent viability. HUVEC = human umbilical vein endothelial cell. These compounds did not inhibit nonendothelial cell proliferation (human foreskin fibroblast IC_{50} > 30 μM).

was prepared. There is adequate space for both bromine substituents to fit into the active site; compound **24** is an inhibitor of 1 nM potency, a 70-fold improvement over compound **4**.

To further explore the active site, analogues were prepared where the phenyl ring was replaced with a heteroaryl ring at the 4-position of the triazole. The active site is reasonably accommodating of large rings such as the benzofuran (**25**). Having a pyridine nitrogen oriented at the 2-position (**26**) also gave a slight enhancement in potency relative to the phenyl compound **4**, while the 3- and 4-pyridyl analogues (**27**, **28**) were substantially less potent. A pyridyl nitrogen at the 2-position would be within 3.4 Å of His339 and may benefit from an additional hydrogen bond. A hydrophobic methyl substituent on the 2-pyridyl ring improved potency particularly when introduced at the 5-position (**30**).

Several of the most potent inhibitors of cobalt-activated hMetAP2 were tested as inhibitors of endothelial cell proliferation, both human (HUVEC) and mouse (MS-1, Table 2). For reference, compound **3** was tested and was found to inhibit cell proliferation in the micromolar range, less potent than would be expected based on the enzyme inhibition data. This is possibly due to low cellular penetration or some other cell specific phenomenon. Another alternative is that manganese, instead of cobalt, is the physiologically relevant metal for hMetAP2,[13] so we also tested our inhibitors against the manganese-activated form of the enzyme (Table 2). The potency order of magnitude is more similar between the manganese-activated enzyme and the inhibition of HUVEC proliferation for several compounds (**3**, **15**, and **16**). However, some compounds are micromolar inhibitors of HUVEC proliferation and are not as potent against the manganese form of the enzyme (**17**, **24**, **25**, and **30**). On the basis of these results, we cannot conclude which metalloenzyme is physiologically relevant; however, we were able to use the cobalt-activated form of the enzyme to progress our program toward the identification of a tool compound for in vivo studies. Compound **24** was identified as a low-micromolar inhibitor of cellular proliferation (HUVEC and MS-1) based on its strong potency against the cobalt-activated enzyme.

One advantage of the 4-aryl-1,2,3-triazole series is the favorable in vivo pharmacokinetic properties, particularly oral exposure. Compound **24** demonstrates low clearance and ~70% oral bioavailability in the rat. Furthermore, following oral administration in the mouse (53 mg/kg), **24** displays systemic exposure at or above the 2 μM level required to maintain potency (MS-1 IC_{50}) for about 8 h postdose (DNAUC = 61 min·kg/L; half-life ~1 h).

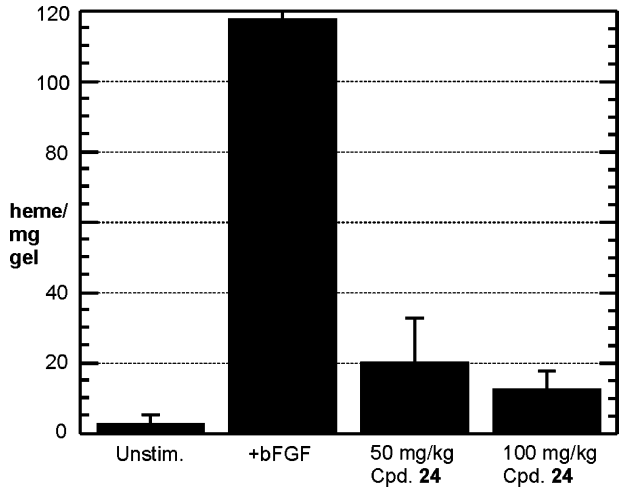

Figure 4. Matrigel plug angiogenesis model. Matrigel plugs were injected subcutaneously in mice, excised after 6 days, and analyzed for hemoglobin content as an index of vascularization. bFGF promotes the vascularization of Matrigel implants in mice as compared to unstimulated control. Oral dosing of compound **24** was performed t.i.d at 50 mg/kg or 100 mg/kg and both where shown to inhibit vascularization. Bars = SEM, $n = 8$, $p = 0.037$ (50 mg/kg), 0.029 (100 mg/kg).

A mouse matrigel model was selected to test the effect a 4-aryl-1,2,3-triazole MetAP2 inhibitor would have on angiogenesis.[27] In this study, mice were injected subcutaneously with growth factor (bFGF) enriched matrigel matrix. Oral (tid) dosing of inhibitor **24** was maintained for 6 days, after which the matrix was excised and a quantitative analysis of vascularization was determined as a direct measure of angiogenesis. Shown in Figure 4, compound **24** inhibited angiogenesis, 83% at 50 mg/kg and 90% at 100 mg/kg. This animal model demonstrates that compound **24**, a 4-aryl-1,2,3-trizaole, is a potent inhibitor of angiogenesis in vivo.

In conclusion, the 4-aryl-1,2,3-triazoles were discovered to be a unique template for the inhibition of the metalloprotease MetAP2. The N-1 and N-2 nitrogens of the triazole structure actively participate in binding to the enzyme active site metals and are key elements for inhibition. Considering their small size, the 4-aryl-1,2,3-triazoles may provide a promising template for the design of new inhibitors of other metalloproteases. Additionally, compound **24** inhibits angiogenesis in a mouse model. The 4-aryl-1,2,3-triazoles are a novel and interesting chemical class which could be further optimized for the treatment of cancer.

Acknowledgment. We thank Dr. Yie-Hwa Chang and St. Louis University as the source of the intellectual property for the type 2 human methionine aminopeptidase, Prof. Jon Clardy and Dr. Cristina Nonato for guidance in crystallizing hMetAP2, and Dr. Martha S. Head for Figure 2.

Supporting Information Available: Method of enzyme inhibition, cellular inhibition, pharmacokinetic analysis, matri-

gel angiogenesis model, crystal structure determination, and refinement statistics, and synthetic procedures and characterization for **3**−**32** are given. This material is available free of charge via the Internet at http://pubs.acs.org.

References

(1) Folkman, J. Angiogenesis in Cancer, Vascular, Rheumatoid and Other Disease. *Nature Med.* **1995**, *1*, 27−31.

(2) Folkman, J. Tumor Angiogenesis: Therapeutic Implications. *New Eng. J. Med.* **1971**, *285*, 1182−1186.

(3) Ingber, D.; Fujita, T.; Kishimoto, S.; Sudo, K.; Kanamaru, T.; Brem, H.; Folkman, J. Synthetic Analogs of Fumagillin that Inhibit Angiogenesis and Suppress Tumor Growth. *Nature* **1990**, *348*, 555−7.

(4) Griffith E. C.; Su Z.; Turk B. E.; Chen S.; Chang Y. H.; Wu Z.; Biemann K.; Liu J. O. Methionine Aminopeptidase (Type 2) is the Common Target for Angiogenesis Inhibitors AGM-1470 and Ovalicin. *Chem. Biol.* **1997**, *4*, 461−471.

(5) Sin, N.; Meng, L.; Wang, M. Q. W.; Wen, J. J.; Bornmann, W. G.; Crews, C. M. The Anti-angiogenic Agent Fumagillin Covalently Binds and Inhibits the Methionine Aminopeptidase, MetAP-2. *Proc. Natl. Acad. Sci. U.S.A.* **1997**, *94*, 6099−6103.

(6) Lowther, W. T.; McMillen, D. A.; Orville, A. M.; Matthews, B. W. The Anti-angiogenic Agent Fumagillin Covalently Modifies a Conserved Active-site Histidine in the Escherichia coli Methionine Aminopeptidase. *Proc. Natl. Acad. Sci. U.S.A.* **1998**, *95*, 12153−12157.

(7) Liu, S.; Widom, J.; Kemp, C. W.; Crews, C. M.; Clardy, J. Structure of Human Methionine Aminopeptidase-2 Complexed with Fumagillin. *Science* **1998**, *282*, 1324−1327.

(8) Griffith, E. C.; Su, Z.; Niwayama, S.; Ramsay, C. A.; Chang, Y.-H.; Liu, J. O. Molecular Recognition of Angiogenesis Inhibitors Fumagillin and Ovalicin by Methionine Aminopeptidase 2. *Proc. Natl. Acad. Sci. U.S.A.* **1998**, *95*, 15183−15188.

(9) Turk, B. E.; Griffith, E. C.; Wolf, S.; Biemann, K.; Chang, Y.-H.; Liu, J. O. Selective Inhibition of Amino-terminal Methionine Processing by TNP-470 and Ovalicin in Endothelial Cells. *Chem. Biol*. **1999**, *6*, 823−833.

(10) Wang, J.; Quan, N.; Henkin, *J. Proc. Am. Assoc. Cancer Res*. **1998**, *39*, 98 (abstract # 664).

(11) Wang, J.; Sheppard, G. S.; Lou, P.; Kawai, M.; BaMaung, N.; Erickson, S. A.; Tucker-Garcia, L.; Park, C.; Bouska, J.; Wang, Y.-C.; Frost, D.; Tapang, P.; Albert, D. H.; Morgan, S. J.; Morowitz, M.; Shusterman, S.; Maris, J. M.; Lesniewski, R.; Henkin, J. Tumor Suppression by a Rationally Designed Reversible Inhibitor of Methionine Aminopeptidase-2. *Cancer Res.* **2003**, *63*, 7861−7869.

(12) Yang, G.; Kirkpatrick, R. B.; Ho, T.; Zhang, G.-F.; Liang, P.-H.; Johanson, K. O.; Casper, D. J.; Doyle, M. L.; Marino, J. P., Jr.; Thompson, S. K.; Chen, W.; Tew, D. G.; Meek, T. D. Steady-State Kinetic Characterization of Substrates and Metal-Ion Specificities of the Full-Length and N−Terminally Truncated Recombinant Human Methionine Aminopeptidases (Type 2). *Biochemistry* **2001**, *40*, 10645−10654.

(13) Wang, J.; Sheppard, G. S.; Lou, P.; Kawai, M.; Park, C.; Egan, D. A.; Schneider, A.; Bouska, J.; Lesniewski, R.; Henkin, J. Physiologically Relevant Metal Cofactor for Methionine Aminopeptidase-2 Is Manganese. *Biochemistry* **2003**, *42*, 5035−5042.

(14) Lowther, W. T.; Zhang, Y.; Sampson, P. B.; Honek, J. F.; Matthews, B. W. Insights into the Mechanism of *Escherichia coli* Methionine Aminopeptidase from the Structural Analysis of Reaction Products and Phosphorus-Based Transition-State Analogues. *Biochemistry* **1999**, *38*, 14810−14819.

(15) Kruger E. A.; Figg W. D. TNP-470: an Angiogenesis Inhibitor in Clinical Development for Cancer. *Expert Opin. Invest. Drugs* **2000**, *9*, 1383−96.

(16) Logothetis, C. J.; Wu, K. K.; Finn, L. D.; Daliani, D.; Figg, W.; Ghaddar, H.; Gutterman, J. U. Phase I Trial of the Angiogenesis Inhibitor TNP-470 for Progressive Androgen-independent Prostate Cancer. *Clin. Cancer Res.* **2001**, *7*, 1198−1203.

(17) Bhargava P.; Marshall J. L.; Rizvi N.; Dahut W.; Yoe J.; Figuera M.; Phipps K.; Ong V. S.; Kato A.; Hawkins M. J. A Phase I and Pharmacokinetic Study of TNP-470 Administered Weekly to Patients with Advanced Cancer. *Clin. Cancer Res.* **1999**, *5*, 1989−95.

(18) Zhou, G.; Tsai, C. W.; Liu, J. O. Fumagalone, a Reversible Inhibitor of Type 2 Methionine Aminopeptidase and Angiogenesis. *J. Med. Chem.* **2003**, *46*, 3452−3454.

(19) Sheppard, G. S.; Wang, J.; Kawai, M.; BaMaung, N. Y.; Craig, R. A.; Erickson, S. A.; Lynch, L.; Patel, J.; Yang, F.; Searle, X. B.; Lou, P.; Park, C.; Kim, K. H.; Henkin, J.; Lesniewski, R. 3-Amino-2-hydroxyamides and Related Compounds as Inhibitors of Methionine Aminopeptidase-2. *Bioorg., Med. Chem. Lett.* **2004**, *14*, 865−868.

(20) Oefner, C.; Douangamath, A.; D'Arcy, A.; Hafeli, S.; Mareque, D.; Sweeney, A. M.; Padilla, J.; Pierau, S.; Schulz, H.; Thormann, M.; Wadman, S.; Dale, G. E. The 1.15 Å Crystal Structure of the Staphylococcus Aureus Methionyl-aminpeptidase and Complexes with Triazole Based Inhibitors. *J. Mol. Biol.* **2003**, *332*, 13−21.

(21) Marino, J. P., Jr.; Thompson, S. K.; Veber, D. F. Substituted Triazole Methionine Aminopeptidase Type 2 Inhibitors, Their Preparation, and Their Therapeutic Use. Patent WO 2002078697, 2002.

(22) Marino, J. P., Jr.; Thompson, S. K.; Veber, D. F. Substituted 1,2,4-Triazole Methionine Aminopeptidase Type 2 Inhibitors, Their Preparation, and Their Therapeutic Use. Patent WO 2002078696, 2002.

(23) Mueller, S.; Liepold, B.; Roth, G. J.; Bestmann, H. J. An Improved One-pot Procedure for the Synthesis of Alkynes from Aldehydes. *Synlett* **1996**, *6*, 521−522.

(24) Tsuchiya, T.; Kato, M.; Sashida, H. Thermal intramolecular cyclization of 2-ethynylpyridine N-ylides to indolizines and cyclazines. *Chem. Pharm. Bull.* **1984**, *32*, 4666−9.

(25) Tanaka, Y.; Velen, S. R.; Miller, S. I. Syntheses and Properties of 1,2,3-Triazoles. *Tetrahedron* **1973**, *29*, 3271−83.

(26) Koradi, R.; Billeter, M.; Wuethrich, K. MOLMOL: A Program for Display and Analysis of Macromolecular Structures. *J. Mol. Graphics* **1996**, *14*, 51−55.

(27) Passaniti, A.; Taylor, R. M.; Pili, R.; Guo, Y.; Long, P. V.; Haney, J. A.; Pauly, R. R.; Grant, D. S.; Martin, G. R. A Simple, Quantitative Method for Assessing Angiogenesis and Antiangiogenic Agents Using Reconstituted Basement Membrane, Heparin, and Fibroblast Growth Factor. *Lab. Invest.* **1992**, *67*, 519−528.

JM050408C